**PASJ:** Publ. Astron. Soc. Japan **54**, 765–773, 2002 October 25


# Detection of Zinc in the Very Metal-Poor Post-AGB Star HR 4049 *

Yoichi TAKEDA,[1] Mudumba PARTHASARATHY,[2,3] Wako AOKI,[2] Yoshifusa ITA,[4]
Yoshikazu NAKADA,[4] Hideyuki IZUMIURA,[5] Kunio NOGUCHI,[2] Masahide TAKADA-HIDAI,[6]
Bun'ei SATO,[5,7] Akito TAJITSU,[5,8] Satoshi HONDA,[2] Satoshi KAWANOMOTO,[2]
Hiroyasu ANDO,[2] and Hiroshi KAROJI[8]

[1]*Komazawa University, Komazawa, Setagaya, Tokyo 154-8525*
*takedayi@cc.nao.ac.jp*
[2]*National Astronomical Observatory, Mitaka, Tokyo 181-8588*
[3]*Indian Institute of Astrophysics, Bangalore 560034, India*
[4]*Institute of Astronomy, The University of Tokyo, Mitaka, Tokyo 181-0015*
[5]*Okayama Astrophysical Observatory, National Astronomical Observatory, Kamogata, Okayama 719-0232*
[6]*Liberal Arts Education Center, Tokai University, Hiratsuka, Kanagawa 259-1292*
[7]*Department of Astronomy, School of Science, The University of Tokyo, Bunkyo-ku, Tokyo 113-0033*
[8]*Subaru Telescope, National Astronomical Observatory of Japan, 650 North A'ohoku Place, Hilo, HI 96720, USA*

(Received 2002 April 22; accepted 2002 July 11)

**Abstract**

We report on the detection of two Zn I lines at 4722.15 Å and 4810.53 Å in the high-quality spectrum of the very metal-poor post-AGB star HR 4049, which was obtained with the High Dispersion Spectrograph attached to the Subaru Telescope. The strengths of these lines indicate an appreciable underabundance of Zn by $\sim -1.3$ dex relative to the Sun. The fact that this volatile element, similarly to others belonging to the same group (e.g., C, N, O, S), does not conform to the extreme depletion ($> 4$ dex) of refractory metals (e.g., Fe), strongly suggests that grain formation has something to do with the origin of the chemical peculiarity. This (not extremely but significantly) subsolar value of [Zn/H] is quantitatively discussed in connection with those of other volatile species, especially with respect to S. We also detected a new Fe II line at 5159.03 Å along with the already known Fe II 4923.93 Å line; based on these two lines the Fe abundance of HR 4049 is determined to be $\sim 2.8$ ([Fe/H] $\sim -4.7$).

**Key words:** astrochemistry — stars: abundances — stars: individual (HR 4049) — stars: post-AGB

## 1. Introduction

HR 4049 (= HD 89353) is a well-known post-AGB star because of its extremely peculiar abundance characteristics: while the abundances of He, C, N, O, and S are not very different from the solar compositions, other elements (e.g., iron-group elements) show ultra-low abundances ($< -4$ dex), as revealed by various spectroscopic studies so far (e.g., Lambert et al. 1988; Takada-Hidai 1990; Waelkens et al. 1991; Bakker et al. 1996).

Several explanations have been proposed for this peculiarity, such as evolution-induced nucleosynthesis, gravitational segregation, accretion of chemically-segregated circumstellar matter, and the removal of the Fe-group elements by fractionation into dust grains followed by mass loss, etc. (see, e.g., Lambert et al. 1988; Bond 1991; Waelkens et al. 1991). Among these, the "depletion" of metals, as a result of selective fractionation into grains, is nowadays considered to be somehow related (at least partly) to the origin of such abundance peculiarities, since the "abundant" elements (He, C, N, O, S) belong to the volatile group of low condensation temperature ($T_c$) in contrast to the "deficient" metals which are the refractory elements with relatively high $T_c$ values. Nevertheless, the detailed mechanism regarding how such an extreme depletion was possible is far from being well understood in a strict sense. What is now required is to accumulate information concerning the reliable abundances of as many elements as possible, so that we can provide theoreticians with observational constraints for developing models and theory to understand the abundance pattern of very metal-poor post-AGB stars.

While there are other post-AGB stars showing similar abundance peculiarities (a good example is HD 52961 which shows quite an analogous tendency to HR 4049; cf. Waelkens et al. 1991), the difficulty involved with the study of HR 4049 lies in its relatively higher temperature ($T_{\rm eff} \sim 7500$ K), as compared to other group members with later spectral type (e.g., $T_{\rm eff}$ of HD 52961 is $\sim 6000$ K; cf. Waelkens et al. 1991). Namely, since the strengths of the spectral lines are even more weakened because of its earlier-type nature, the lines available for abundance determinations are quite limited (for example, its metallicity has so far been derived based on only one Fe II line; cf. Waelkens et al. 1991), and spectrum data with sufficiently high quality are indispensable.

Considering this situation, we recently observed HR 4049 with the Subaru Telescope and obtained a spectrum of satisfactorily high S/N ratio. In this paper, we report on our new findings, based on this high-quality spectrum, regarding the following two motivations of special interest:

* Based on data collected at Subaru Telescope, which is operated by the National Astronomical Observatory.

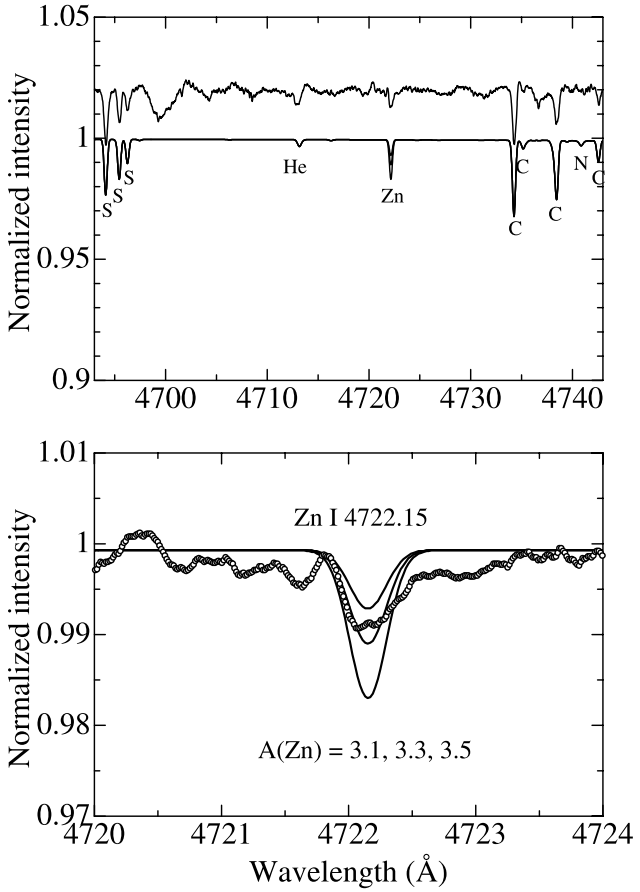


**Fig. 1.** Spectral features around the Zn I line at 4722.15 Å. While the global appearance in this spectral region is presented in the upper panel, the lower panel shows its detailed line profile on a much more magnified scale. The observed spectrum shown here (solid line in the upper panel, and open circles in the lower panel) is that of the smoothed one (cf. section 2). Three theoretical spectra (solid lines) corresponding to the Zn abundance of 3.1, 3.3, and 3.5 (i.e., the finally adopted mean abundance along with the perturbations of $\pm 0.2$ dex) are also depicted. See section 4 for more details regarding the theoretical spectrum synthesis. A vertical offset by +0.02 is applied to the observed spectrum in the upper panel.

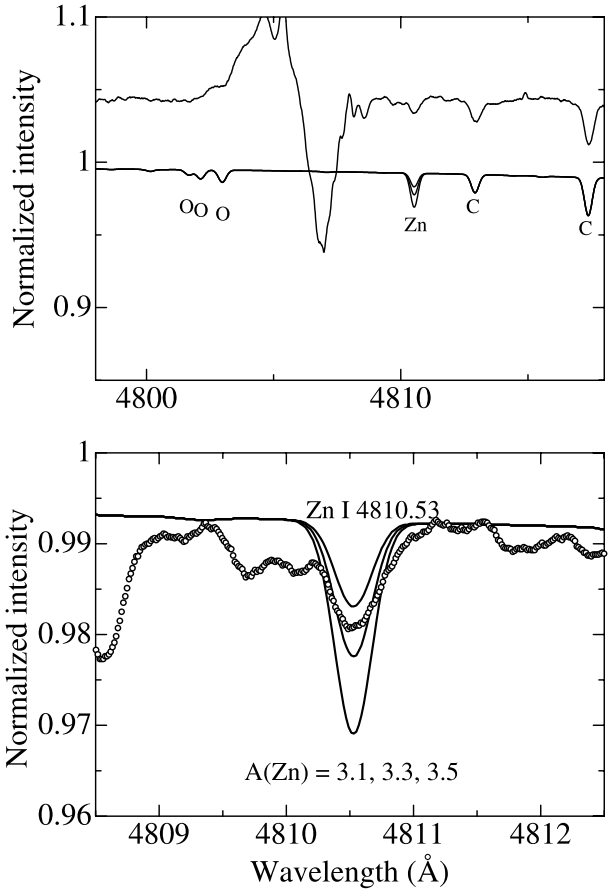


**Fig. 2.** Observed spectral features around the Zn I line at 4810.53 Å, along with the theoretical spectra computed with Zn abundances of 3.1, 3.3, and 3.5. A vertical offset by +0.05 is applied to the observed spectrum in the upper panel. The spike feature seen in 4802–4807 Å is nothing but that due to defects (bad pixels) on the CCD. Otherwise, the same as in figure 1.

*(1) Search for lines of zinc.*

Although this is another element belonging to the volatile group (such as C, N, O, and S) owing to its low $T_c$ of 660 K (e.g., Wasson 1985), its detection in the spectrum of HR 4049 has never been reported. If Zn could be confirmed to share the same property as that of other volatile elements, such as was established for HD 52961 by Van Winckel et al. (1992) and for HD 44179 by Waelkens et al. (1996), this would be another evidence supporting the fractionation hypothesis.

*(2) Search for new lines of Fe-group elements.*

As mentioned above, only one line (Fe II 4923.93) has so far been available for evaluating the metallicity (i.e., abundances of extremely deficient metals), which is evidently insufficient. Toward a reliable establishment of to which extent these refractory elements are depleted, the detection of more lines of such elements is highly desired. Hence, we confined ourselves to searching for new lines of Fe II and Ti II, which are typically observed in normal F-supergiants.

## 2. Observational Data

The observation was carried out on 2002 February 1 during a test observing run for the HDS (High Dispersion Spectrograph) of the 8.2 m Subaru Telescope (Noguchi et al. 2002). Three frames of 120 s exposure were obtained with the standard setup for the blue region, which covers 3540–5260 Å with a resolution of $\sim 60000$.

The data reduction was performed in a standard manner using the IRAF **`echelle`** package. Since the existence of strong and broad hydrogen Balmer absorption lines in the spectrum makes it difficult to determine the continuum level accurately, we first corrected the echelle blaze profiles of the object spectrum using the profiles of flat data, and then applied the IRAF **`continuum`** routine. Though the uncertainty in the continuum level estimation is still large ($\sim 10\%$) around the broad absorption features, we can estimate the local continuum for weak absorption lines for which an abundance analysis was performed in the present work. The S/N ratio of the

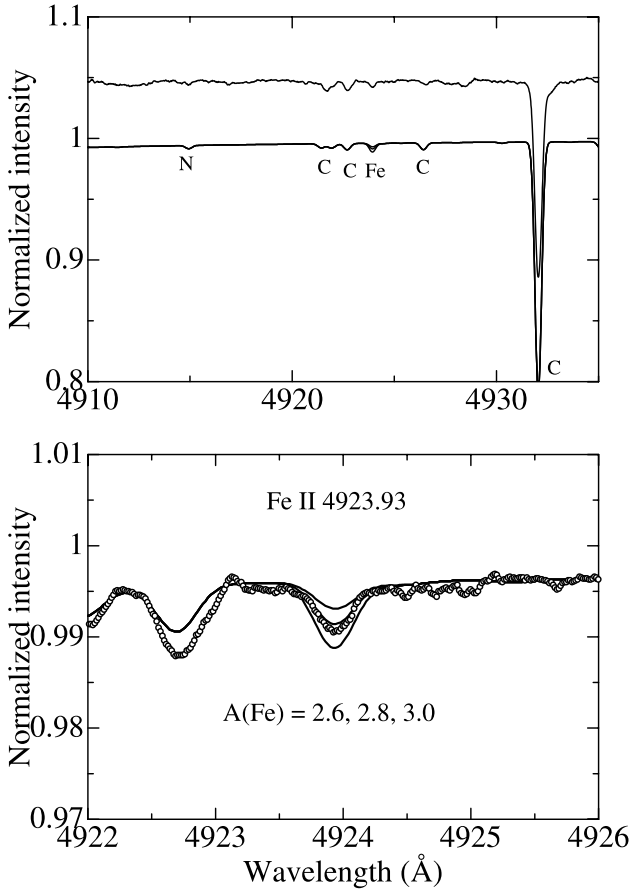


**Fig. 3.** Observed spectral features around the Fe II line at 4923.93 Å, along with the theoretical spectra computed with the Fe abundances of 2.6, 2.8, and 3.0. A vertical offset by +0.05 is applied to the observed spectrum in the upper panel. Otherwise, the same as in figure 1.

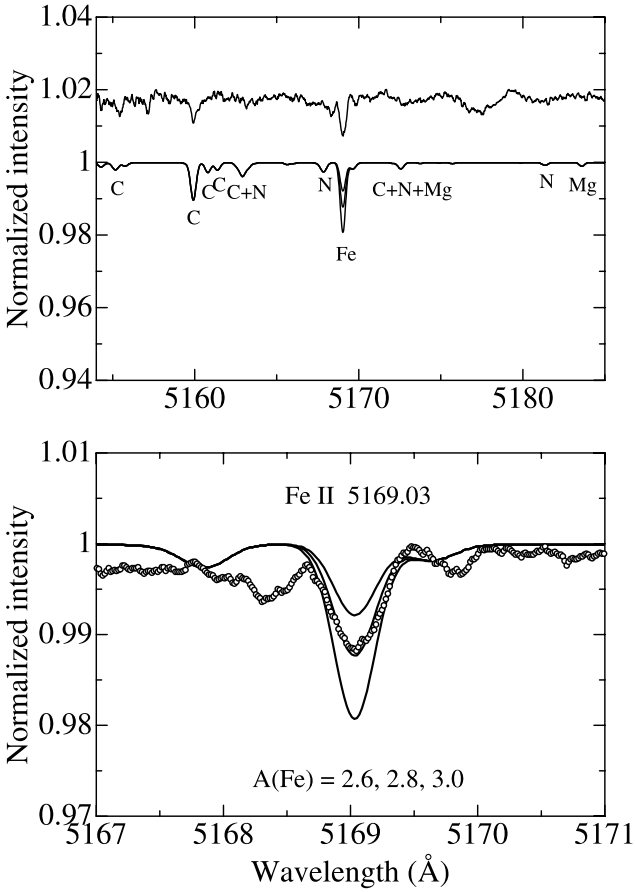


**Fig. 4.** Observed spectral features around the Fe II line at 5169.03 Å, along with the theoretical spectra computed with the Fe abundances of 2.6, 2.8, and 3.0. A vertical offset by +0.02 is applied to the observed spectrum in the upper panel. Otherwise, the same as in figure 1.

final spectrum, obtained by coadding the three spectra of 120 s exposure, turned out to be 400–500 in the wavelength region longward of 4000 Å. We further smoothed the spectrum by taking the running mean over 11 pixels (i.e., convolving the spectrum with a box function of 10-pixel width) with the help of the **splot** task in IRAF. This actually improved the local S/N ratio (thus making the line-identification and equivalent-width measurement easier) without significantly degrading the stellar line spectra, whose widths ($\sim 25\,\mathrm{km\,s^{-1}}$) are intrinsically broader than that of the smoothing function ($\sim 10\,\mathrm{km\,s^{-1}}$). The smoothed spectrum was used throughout this study.

## 3. Search for the Lines

In order to find new lines of our target elements (i.e., Zn, Fe, and Ti in the present case), we computed the theoretical equivalent widths for all available lines of each species in the wavelength region of 3540–5260 Å on the standard atmospheric model ($T_{\rm eff} = 7500$ K, $\log g = 2.0$, and [M/H] = −5; cf. section 4) for appropriately chosen trial abundances. Regarding the data of the spectral lines, we invoked Kurucz and Bell's (1995) extensive compilation.

If Zn has an abundance near to the solar value of $A_\odot(\mathrm{Zn})$[1] = 4.60 (Anders, Grevesse 1989), our calculation suggested that three Zn I lines at 4680.13, 4722.15, and 4810.53 Å should definitely be detectable with equivalent widths on the order of several tens of mÅ. Having inspected the spectrum, we confidently confirmed the detections of the latter two lines (Zn I 4722.15 and 4810.53), as demonstrated in figures 1 and 2. However, we could not definitely identify the 4680.13 line in this analysis, the weakest among the three, because of its being blended with another unknown feature. The strong bump conspicuously seen in 4802–4807 Å (figure 2) is due to the fact that the corresponding echelle order crosses the closely concentrated $\sim 5$ bad columns (i.e., trains of bad pixels) of the CCD at this spectrum portion. We confirmed, however, that these defects do not affect the wavelength region longward of 4809 Å, and thus there is no significant influence on the measurement of the Zn I 4810.53 line.

Regarding Fe, three Fe II lines at 4923.93, 5018.44, 5169.03 Å were selected as probably detectable candidates (i.e., $W_\lambda \gtrsim 1$ mÅ), even for the extremely low Fe abundance of $A(\mathrm{Fe}) \sim 2.5$ (i.e., deficient by 5 dex relative to the solar abundance of 7.50; cf. Grevesse, Sauval 1999). Among these we could identify the 4923.93 Å and 5169.03 Å lines, as shown in

[1] In this paper we express the logarithmic abundance for an element by $A$(element), which is defined as $A(\mathrm{element}) \equiv \log(N_{\rm element}/N_{\rm H}) + 12$.

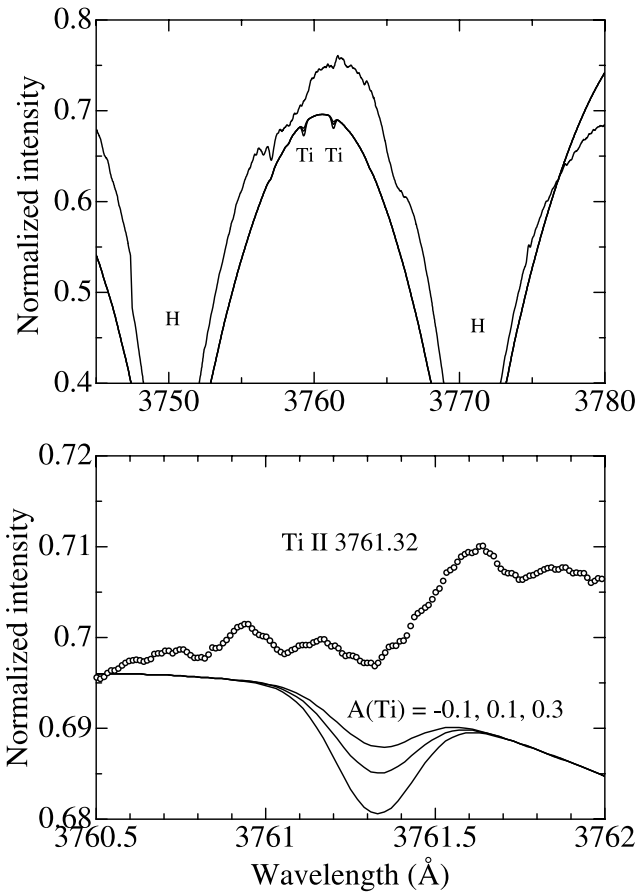


**Fig. 5.** Observed spectral features around the Ti II line at 3761.32 Å, along with the theoretical spectra computed with the Ti abundances of −0.1, 0.1, and 0.3. Because of the difficulty in the normalization due to the blending of strong Balmer lines, the observed spectrum is multiplied by arbitrary factors in the upper as well as lower panels, in order to bring both spectra close to each other for an adequate comparison. Otherwise, the same as in figure 1.

figures 3 and 4; the former is a reconfirmation of Waelkens et al.'s (1991) detection, while the latter is the discovery of another new Fe II line in this star. Unfortunately, the 5018.44 line could not be detected because it is blended with the C I (at 5018.10 Å) and O I (at 5018.78 Å) lines.

Then, our calculation suggested that only two Ti II lines at 3759.30 Å and 3761.32 Å may be observable with equivalent widths of a few mÅ, even at an ultra-low Ti abundance of $A$(Ti) ∼ 0 (drastically underabundant by ∼ 5 dex relative to the solar value of 4.99; cf. Anders, Grevesse 1989). Unfortunately, these lines are located in the spectral region conspicuously influenced by the overlapped wings of the Balmer lines. Nevertheless, as displayed in figure 5, a marginal (though uncertain) sign of the 3761.32 Å line might as well be observed almost at the detectability limit, while the 3759.30 Å line can not be seen because of the spurious broad feature at this wavelength.

## 4. Abundance Determination

We measured the equivalent widths of the detected five lines (cf. section 3) by the Gaussian fitting method in order to determine the abundances of Zn, Fe, and Ti. In addition, we also evaluated the strengths of three S I lines at 4694–6 Å to establish the abundance of S for the discussion in subsection 5.2. Regarding the model atmosphere, we adopted Kurucz's (1993) ATLAS9 model with atmospheric parameters of $T_{\rm eff}$ = 7500 K, $\log g$ = 2.0, and [M/H] = −5.0, following Monier and Parthasarathy (1999). The line data (wavelengths, excitation potentials, and $gf$ values) were taken from Kurucz and Bell (1995), and the microturbulent velocity was assumed to be 5 km s$^{-1}$ according to Waelkens et al. (1991). We used the WIDTH9 program (Kurucz 1993), which was modified by Y. T. in various respects, for abundance determinations. The resulting abundances, along with the equivalent widths and the atomic data, are given in table 1. Averaging the results of two lines in the cases of Zn and Fe, we obtain $A$(Zn) = 3.3 and $A$(Fe) = 2.8; i.e., [Zn/H] = −1.3 and [Fe/H] = −4.7 in terms of the differential abundances relative to the Sun (cf. section 3).

Also, we roughly estimated the equivalent width of the Ti II 3761.32 line to be ∼ 3 mÅ, which yields $A$(Ti) ∼ 0.1 ([Ti/H] ∼ −4.9). However, owing to its large uncertainty, this value should be viewed with caution.

In table 1 we also show the results of an analysis of the S I lines, which suggest the mean abundance of $A$(S) = 6.7; i.e., [S/H] = −0.5, as compared to the solar S abundance of 7.21 (Anders, Grevesse 1989).

In figures 1–5, the theoretical spectra corresponding to these abundance solutions (as well as the spectra corresponding to the abundance perturbations of ±0.2 dex) are depicted along with the observed spectrum. Since it was found that the $gf$ values of many C I lines included in the compilation of Kurucz and Bell (1995) contain rather large errors, we replaced their data of important C I lines with those of Hibbert et al. (1993) or with the empirically adjusted values in the spectrum synthesis shown in these figures. These theoretical spectra are convolved with a Gaussian broadening profile of FWHM = 20 km s$^{-1}$ (i.e., $e$-folding half-width of 12 km s$^{-1}$), by which we found that the actual line-widths of HR 4049 can be well reproduced. Regarding the other volatile elements, we assumed [He/H] = +0.3, [C/H] = −0.3, [N/H] = 0.0, [O/H] = −0.3, and [S/H] = −0.5, based on our supplementary analysis of the lines of these elements identified in our violet–green spectra (cf. Appendix).

In table 1 are also given the abundance variations in response to changing the $T_{\rm eff}$ and $\log g$ values by ±250 K and ±0.5 dex, which we regard as being the typical uncertainties in these parameters. The choice of the microturbulent velocity is practically irrelevant in the present case of very weak lines. Similarly, the uncertainty in the metallicity of the model hardly affects the abundances ([M/H] = −4 and −5 models yields essentially the same results). An inspection of table 1 indicates that uncertainties of ∼ ±0.1–0.2 dex may be involved in the solutions, caused by ambiguities in $T_{\rm eff}$ and $\log g$.

The errors in the measured equivalent widths of the Zn I and Fe II lines from the viewpoint of the photometric accuracy may be estimated as ±0.2–0.3 mÅ (i.e., ±5–10% of $W_\lambda$)

**Table 1.** Line parameters, equivalent widths, and the resulting abundances of Zn, Fe, Ti, and S.

| Species | $\lambda$ (Å) | $\chi_{\rm low}$ (eV) | $\log gf$ | $W_\lambda$ (mÅ) | $A$(element) | $\Delta_T^-$ | $\Delta_T^+$ | $\Delta_g^-$ | $\Delta_g^+$ | $\Delta_v^-$ | $\Delta_v^+$ |
|---|---|---|---|---|---|---|---|---|---|---|---|
| Zn I | 4722.153 | 4.030 | −0.338 | 3.4 | 3.25 | −0.21 | +0.24 | +0.10 | −0.07 | 0.00 | 0.00 |
| Zn I | 4810.528 | 4.078 | −0.137 | 6.4 | 3.36 | −0.21 | +0.24 | +0.10 | −0.07 | +0.01 | 0.00 |
| Fe II | 4923.927 | 2.891 | −1.320 | 1.6 | 2.76 | −0.09 | +0.11 | −0.10 | +0.12 | 0.00 | 0.00 |
| Fe II | 5169.033 | 2.891 | −0.870 | 4.8 | 2.79 | −0.09 | +0.11 | −0.10 | +0.12 | 0.00 | 0.00 |
| Ti II | 3761.323 | 0.574 | +0.100 | (3:) | (0.06:) | −0.15 | +0.16 | −0.12 | +0.14 | 0.00 | 0.00 |
| S I | 4694.113 | 6.524 | −1.770 | 10.4 | 6.78 | −0.14 | +0.18 | +0.07 | −0.03 | +0.01 | −0.01 |
| S I | 4695.443 | 6.524 | −1.920 | 5.8 | 6.67 | −0.14 | +0.18 | +0.07 | −0.03 | +0.01 | 0.00 |
| S I | 4696.252 | 6.524 | −2.140 | 3.2 | 6.63 | −0.14 | +0.18 | +0.07 | −0.03 | 0.00 | 0.00 |

Note. The line parameters (species, wavelengths, lower excitation potentials, and $gf$ values) are given in columns 1–4, followed by the measured equivalent width in the 5th column. The resulting abundances, which were determined on the fiducial atmospheric model ($T_{\rm eff}$ = 7500 K, $\log g$ = 2.0, [X/H] = −5.0) along with the microturbulent velocity of $v_{\rm t}$ = 5 km s$^{-1}$, are presented in the 6th column. Since the results for the Ti II 3761.32 Å line (shown with parentheses) suffer large uncertainties, they should be viewed with caution. Columns 7–12 show the abundance variations caused by changing the standard values of $T_{\rm eff}$ (7500 K), $\log g$ (2.0), and $v_{\rm t}$ (5 km s$^{-1}$) by −250 K ($\Delta_T^-$), +250 K ($\Delta_T^+$), −0.5 ($\Delta_g^-$), +0.5 ($\Delta_g^+$), −2 km s$^{-1}$ ($\Delta_v^-$), and +2 km s$^{-1}$ ($\Delta_v^+$), respectively. The original references for the sources of the $gf$ values, which we adopted from the compilation of Kurucz and Bell (1995), are as follows: Warner (1968) for the Zn I lines, Fuhr et al. (1988) for the Fe II lines, Martin et al. (1988) for the Ti II line, and Wiese et al. (1966) for the S I lines.

by applying Cayrel's (1988) formula to our case (FWHM of $w \sim 0.4$ Å, pixel size of $\delta x \sim 0.01$ Å, and photometric error of $\epsilon \sim 1/400$). An inspection of figures 1–4 suggests, however, that actual errors may be larger than this (presumably ±20–30% may be a more reasonable estimate) because of the difficulty in determining the continuum level. Hence, errors in the $W_\lambda$ values may lead to abundance uncertainties of $\sim \pm 0.1$ dex.

Summarizing what has been described above, we consider that ambiguities amounting to $\sim \pm 0.2$ dex may be involved in our abundance results of Zn and Fe. Keeping this in mind, we conclude [Zn/H] $\sim -1.3$ and [Fe/H] $\sim -4.7$, as the abundances of these elements in the photosphere of HR 4049.

## 5. Discussion

### 5.1. Fe Group

According to the results of the Fe (and Ti) lines described in the previous section, [Fe/H] $\sim -4.7$ (and [Ti/H] $\sim -4.9$, though uncertain), we may state that the deficiencies of these Fe-group elements are in the range between $\sim -4.5$ dex and $\sim -5$ dex, which almost confirms the conclusion ([Fe/H] = −4.8) of Waelkens et al. (1991). When we consider the difference in the reference solar Fe abundance between ours and theirs [i.e., we used Grevesse and Sauval's (1999) value of 7.50, while they adopted Anders and Grevesse's (1989) value of 7.67], the coincidence becomes even better.

### 5.2. Zinc

#### 5.2.1. Evidence for the grain-related depletion

The result of [Zn/H] $\sim -1.3$ (±0.2) is considered to be significant. Namely, zinc (a volatile element of low $T_{\rm c}$ similar to C, N, O, and S) evidently does not conform to the extreme depletion of the iron group elements (i.e., refractory elements with high $T_{\rm c}$ which are apt to be fractionated into grains) in spite of the similarity in the atomic number (or mass). Hence, as in the case of HD 52961 and HD 44179, which are two other very metal-poor post-AGB stars in which Zn is detected (Van Winckel et al. 1992; Waelkens et al. 1996), this fact lends support to the hypothesis that the depletion of those metals as a result of the chemical fractionation into solid particles (or dusts) is the cause of the remarkable peculiarity in the photospheric abundances of HR 4049, though little is known about the detailed mechanism of how this could actually be accomplished.

#### 5.2.2. Comparison with other volatile elements

We notice, however, that the abundance of Zn in HR 4049 is somewhat different from those of other volatile members (He, C, N, O, and S) which have near-solar compositions within the range of $+0.3 \gtrsim$ [X/H] $\gtrsim -0.5$ (cf. Appendix). Namely, Zn shows an appreciable deficiency of −1.3 dex (though not so extreme as in the case of refractory species) in spite of its low $T_{\rm c}$, which is not so conspicuously observed in other volatile species.

Let us pay attention to the marked abundance difference amounting to 0.8 dex between Zn ([Zn/H] = −1.3) and S ([S/H] = −0.5), both of which have a quite similar $T_{\rm c}$ value of $\sim$ 650 K (e.g., Wasson 1985) and thus nearly the same properties in terms of the fractionation into grains. Presumably, this supersolar [S/Zn] value may (at least partly) be attributed to the primordial abundances of S and Zn. That is, since Zn and S are considered to be free from any significant depletion (because of their volatile nature) or from the effect of nuclear processing during stellar evolution (according to the canonical stellar evolution theory), it may be reasonable to assume that the initial abundances of these elements are retained. Then, HR 4049 would have originally been a typical halo star of [Fe/H] ($\simeq$ [Zn/H]) $\sim -1.3$, since [Zn/Fe] $\simeq 0$ is known to hold over a wide range of metallicity (cf. Sneden et al. 1991).

**Table 2.** Literature abundances of Fe, Zn, and S for RV Tau variables and post-AGB stars.

| Star | [Fe/H] | [Zn/H] | [S/H] | [S/Zn] | [Zn/Fe] | [S/Fe] | Reference |
|---|---|---|---|---|---|---|---|
| [RV Tauri-type variables] | | | | | | | |
| SS Gem | −0.87 | +0.02 | −0.42 | −0.44 | +0.89 | +0.45 | GLG97b |
| CT Ori | −1.87 | −0.58 | −0.53 | +0.05 | +1.29 | +1.34 | GLG97b |
| IW Car | −1.06 | −0.04 | +0.36 | +0.40 | +1.02 | +1.42 | GRL94 |
| RU Cen | −1.90 | −1.00 | −0.68 | +0.32 | +0.90 | +1.22 | MVW |
| SX Cen | −1.15 | −0.54 | −0.08 | +0.46 | +0.61 | +1.07 | MVW |
| AC Her | −1.69 | −1.02 | −0.75 | +0.27 | +0.67 | +0.94 | VWWMUB |
| AC Her | −1.40 | −0.93 | −0.37 | +0.56 | +0.47 | +1.03 | GLG98 |
| AC Her | −0.82 | −0.12 | −0.25 | +0.13 | +0.70 | +0.57 | KP |
| V360 Cyg | −1.40 | −1.36 | −0.88 | +0.48 | +0.04 | +0.52 | GLG98 |
| EP Lyr | −1.80 | −0.70 | −0.61 | +0.09 | +1.10 | +1.19 | GLG97a |
| R Sge | −0.50 | −0.19 | +0.37 | +0.56 | +0.31 | +0.87 | GLG97a |
| DY Ori | −2.30 | +0.21 | +0.16 | −0.05 | +2.51 | +2.46 | GLG97a |
| DS Aqr | −1.14 | −1.07 | −0.82 | +0.25 | +0.07 | +0.32 | GLG00 |
| UY Ara | −1.02 | −0.29 | +0.01 | +0.30 | +0.73 | +1.03 | GLG00 |
| TW Cam | −0.50 | −0.34 | −0.05 | +0.29 | +0.16 | +0.45 | GLG00 |
| BT Lib | −1.18 | −1.06 | −0.76 | +0.30 | +0.12 | +0.42 | GLG00 |
| TT Oph | −0.85 | −0.71 | +0.01 | +0.72 | +0.14 | +0.86 | GLG00 |
| U Mon | −0.79 | −0.71 | −0.15 | +0.56 | +0.08 | +0.64 | GLG00 |
| U Mon | −0.68 | −0.49 | −0.09 | +0.40 | +0.19 | +0.59 | KP |
| RV Tau | +0.08* | +0.17 | +0.90 | +0.73 | +0.09 | +0.82 | KP |
| AD Aql | −2.12 | −0.12 | −0.03 | +0.09 | +2.00 | +2.09 | GLG98 |
| ST Pup† | −1.47 | −0.06 | −0.18 | −0.12 | +1.41 | +1.29 | GW |
| [High-latitude supergiants (possible post-AGB stars)] | | | | | | | |
| HD 46703 | −1.7 | −1.3 | −0.4 | +0.9 | +0.4 | +1.3 | GRL94‡ |
| HR 7671 | −1.11 | −0.85 | −0.95 | −0.10 | +0.26 | +0.16 | LBL |
| 89 Her | −0.41 | −0.38 | −0.26 | +0.12 | +0.03 | +0.15 | LBL |
| HD 161796 | −0.32 | +0.24 | +0.41 | +0.17 | +0.56 | +0.73 | LBL |
| HR 6144 | −0.36 | +0.11 | +0.03 | −0.08 | +0.47 | +0.39 | LBL |
| [Very metal-poor post-AGB stars] | | | | | | | |
| HD 52961 | −4.8 | −1.5 | −1.0 | +0.5 | +3.3 | +3.8 | WVWB |
| HD 44179 | −3.3 | −0.6 | −0.3 | +0.3 | +2.7 | +3.0 | WVWB |
| HR 4049 | −4.7 | −1.3 | −0.5 | +0.8 | +3.4 | +4.2 | this study |

Note. Given are the logarithmic abundance ratios for Fe, Zn, and S relative to the Sun taken from various literature, along with the ratios of S-to-Zn, Zn-to-Fe, and S-to-Fe (defined, e.g., as [S/Zn] ≡ [S/H] − [Zn/H], and so on). The keys to the references of the data sources are as follows: GRL94 — Giridhar et al. (1994); GLG97a — Gonzalez et al. (1997a); GLG97b — Gonzalez et al. (1997b); GLG98 — Giridhar et al. (1998); GLG00 — Giridhar et al. (2000); GW — Gonzalez and Wallerstein (1996); WVWB — Waelkens et al. (1996); VWWMUB — Van Winckel et al. (1998); MVW — Maas et al. (2002); LBL — Luck et al. (1990); KP — Klochkova and Panchuk (1998).

* Giridhar et al. (2000) reports an appreciably lower [Fe/H] value of −0.43 for this star.

† This star is a W Vir-type Cepheid, but is suspected to be a post-AGB star from its abundance characteristics similar to RV Tau variables.

‡ See their table 5.

Also, because S is known to show a mildly supersolar [S/Fe] ratio of $\sim$0.3–0.5 (reflecting the nature of $\alpha$-process elements) in typical galactic halo stars with $-1.5 \lesssim$ [Fe/H] $\lesssim -1$ (see, e.g., Takada-Hidai et al. 2002), the initial positive value of [S/Zn] ($\simeq$ [S/Fe]) may have remained unchanged during the past stellar evolution.

*5.2.3. Zn and S in post-AGB and related stars*

In order to check this interpretation, we collected from various literature the published values of [Zn/H] and [S/H] for RV Tau variables, high-latitude A–F supergiants (post-AGB candidates), and very metal-poor post-AGB stars, all of which are known to share qualitatively the same properties of chemical abundances (i.e., depletion of refractory metals while non-depletion of volatile species), as summarized in table 2. The [S/Zn] vs. [Zn/H] plots based on these data are shown in figure 6. In view of the above discussion, this relation would look similar to that of [S/Fe] vs. [Fe/H] for galactic disk/halo stars. As can be recognized from this figure, a tendency can be seen that [S/Zn] decreases with an increase

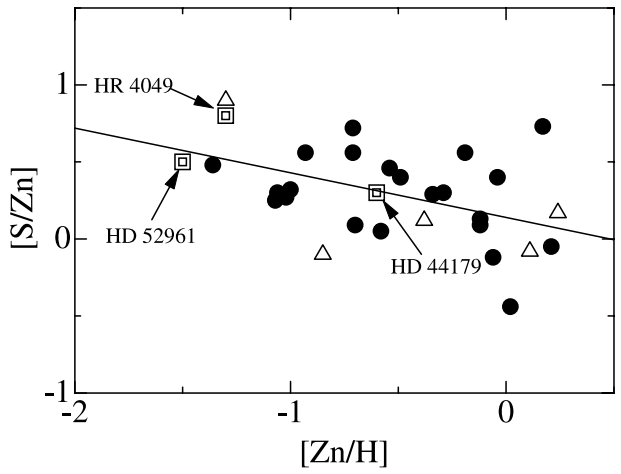


**Fig. 6.** [S/Zn] vs. [Zn/H] relation constructed from various literature data given in table 2. Filled circles — RV Tau variables; open triangles — high-latitude supergiants; double squares — very metal-poor post-AGB stars. The solid line is the linear-regression line determined from these data, [S/Zn] = −0.29 (±0.10) [Zn/H] + 0.14 (±0.07).

in [Zn/H] (though with a large diversity); i.e., from a positive ($\sim +0.5$–1) [S/Zn] at [Zn/H] $\sim -1.5$ to [S/Zn] $\sim 0$ at [Zn/H] $\sim 0$. Although the scatter is rather large, we may state that the negative slope is statistically significant, since the correlation coefficient between [Zn/H] and [S/Zn] is −0.48 and the linear-regression line determined from these data is [S/Zn] = −0.29 (±0.10) [Zn/H] + 0.14 (±0.07) (cf. figure 6). Hence, this trend is *qualitatively* the same as that observed in the [S/Fe] vs. [Fe/H] relation in galactic solar-type stars.

Now, since we can see from figure 6 that HR 4049 appears to follow this general trend, the speculation mentioned above may be reasonable; i.e., because the primordial abundances of Zn and S in HR 4049 (which would have originally been a typical population II star of [Fe/H] $\sim -1.3$) are expected to be mostly retained in its atmosphere, the currently observed largely positive [S/Zn] value may be interpreted as reflecting the initial trend of supersolar [S/Fe] values in halo stars.

*5.2.4. Possible anomaly in volatile species*

From a quantitative point of view, however, we feel that the actual situation may be more complicated than such a simple picture. That is, the [S/Zn] value of $\sim +0.8$ appears to be somewhat too large compared to the typical [S/Fe] value (0.3–0.5) of halo stars ([Fe/H] $\sim -1.5$); i.e., it appears rather difficult to reduce this value significantly, since the sensitivities of Zn I and S I lines to atmospheric parameters are quite similar (cf. table 1) and the $gf$ values we adopted are sufficiently reliable being free from significant systematic errors.[2] Considering that such markedly large [S/Zn] values are observed in not a few stars of a similar group (cf. figure 6), it would be more reasonable to assume that such stars, including HR 4049, may have undergone some alteration of the abundances of either Zn or S.

[2] We confirmed based on the analysis of solar spectral lines that those $gf$ values satisfactorily reproduced our reference solar abundances adopted from Anders and Grevesse (1989).

For example, some kind of special (i.e., non-canonical) nucleosynthesis mechanism might as well be considered, such as the one speculated by Bond and Luck (1987); i.e., the synthesis of $^{32}$S during a violent He-core flash at the tip of the red-giant branch. Alternatively, considering that several RV Tau stars in table 2 show similar [Zn/H] values to [Fe/H] ones, the possibility that Zn may be partially depleted into dust grains would have to be kept in mind.

Also, if the "fossil" interpretation for Zn is correct, considerably supersolar ratios of [C/Zn], [N/Zn], [O/Zn] amounting up to $\sim +1$ imply a considerable enrichment of C, N, and O by the similar extent, since [C/Fe], [N/Fe], [O/Fe] values of mildly metal-poor stars do not largely deviate from zero (except for [O/Fe] which is moderately supersolar). Though, admittedly, the abundances of these light elements can be altered by the stellar evolution (i.e., nuclear-processing and dredge-up during the course of AGB and post-AGB evolution), whether such an opportune enrichment process that brings CNO into near-solar surface abundances exists is yet to be investigated.

## Appendix. Analysis of the Lines of Other Elements

In connection with the discussion on Zn and S presented in subsection 5.2, we require information concerning the abundances of other volatile elements. In this Appendix we describe our supplementary analysis on the abundances of He, C, N, O, and Ca carried out for this purpose, since lines of these elements were clearly identified in our 2002 February spectrum used in this study.

The model atmosphere adopted as well as the method of abundance determination is basically the same as described in section 4. Also, except for the case of C I lines (see below), we invoked the $gf$ values (along with the damping parameters) taken from the compilation of Kurucz and Bell (1995). The results are summarized in table 3, from which we obtained $\langle A\rangle_{\rm He} = 11.31$, $\langle A\rangle_{\rm C} = 8.23$, $\langle A\rangle_{\rm N} = 8.05$, $\langle A\rangle_{\rm O} = 8.62$, and $\langle A\rangle_{\rm Ca} = 0.26$ as the abundances of these elements in HR 4049. By comparing these with the solar abundances taken from Anders and Grevesse (1989) (10.99, 8.56, 8.05, 8.93, and 6.36, respectively), we conclude [He/H] = +0.3, [C/H] = −0.3, [N/H] = 0.0, [O/H] = −0.3, and [Ca/H] = −6.1. Additional comments related to the choice of the lines and the $gf$ values are given below:

*Helium* These $gf$ values originally stem from Wiese et al. (1966). Although the He I line at 4713 Å is also clearly seen (cf. figure 1), this line was not included because a reliable measurement of line strength was rather difficult due to some distortion (blending?) of the feature.

*Carbon* We identified and measured about sixty lines of C I. However, the $gf$ values compiled by Kurucz and Bell (1995) were taken from various sources of diverse quality. Hence, having decided to exclusively invoke the recently calculated $gf$ values of Hibbert et al. (1993) (length form), we restricted our carbon analysis only to those 19 C I lines, for which these data are available. We do not find any systematic

**Table 3.** Line data and the resulting abundances of He, C, N, O, and Ca.

| Species | λ (Å) | $\chi_{low}$ (eV) | log $gf$ | $W_\lambda$ (mÅ) | $A$(element) | $\Delta_T^-$ | $\Delta_T^+$ | $\Delta_g^-$ | $\Delta_g^+$ | $\Delta_v^-$ | $\Delta_v^+$ |
|---|---|---|---|---|---|---|---|---|---|---|---|
| He I | 4026.18 | 20.96 | −2.62 | 12.7 | 11.22 | +0.40 | −0.30 | −0.25 | +0.37 | +0.01 | −0.01 |
| | 4026.19 | | −0.70 | | | | | | | | |
| | 4026.19 | | −1.45 | | | | | | | | |
| | 4026.20 | | −1.45 | | | | | | | | |
| | 4026.20 | | −0.97 | | | | | | | | |
| | 4026.36 | | −1.32 | | | | | | | | |
| He I | 4471.47 | 20.96 | −2.20 | 13.5 | 11.40 | +0.40 | −0.30 | −0.24 | +0.32 | +0.02 | −0.02 |
| | 4471.47 | | −1.03 | | | | | | | | |
| | 4471.47 | | −0.28 | | | | | | | | |
| | 4471.49 | | −1.03 | | | | | | | | |
| | 4471.49 | | −0.55 | | | | | | | | |
| | 4471.68 | | −0.90 | | | | | | | | |
| C I | 4762.31 | 7.48 | −2.35 | 85.7 | 8.32 | −0.08 | +0.13 | +0.03 | +0.02 | +0.03 | −0.01 |
| | 4762.53 | | −2.23 | | | | | | | | |
| C I | 4766.67 | 7.48 | −2.51 | 25.6 | 8.28 | −0.08 | +0.13 | +0.03 | +0.01 | +0.02 | −0.01 |
| C I | 4770.03 | 7.48 | −2.33 | 34.3 | 8.24 | −0.08 | +0.13 | +0.03 | +0.02 | +0.03 | −0.02 |
| C I | 4771.74 | 7.49 | −1.76 | 91.7 | 8.24 | −0.08 | +0.13 | +0.02 | +0.02 | +0.10 | −0.06 |
| C I | 4775.90 | 7.49 | −2.19 | 45.2 | 8.25 | −0.08 | +0.13 | +0.03 | +0.02 | +0.04 | −0.02 |
| C I | 4812.92 | 7.48 | −3.23 | 7.8 | 8.45 | −0.08 | +0.13 | +0.03 | +0.02 | +0.01 | 0.00 |
| C I | 4817.37 | 7.48 | −2.89 | 12.9 | 8.34 | −0.08 | +0.13 | +0.03 | +0.02 | +0.01 | −0.01 |
| C I | 4826.80 | 7.49 | −3.05 | 9.6 | 8.38 | −0.08 | +0.13 | +0.03 | +0.02 | +0.01 | 0.00 |
| C I | 4888.94 | 7.48 | −3.82 | 4.2 | 8.78 | −0.08 | +0.13 | +0.02 | +0.02 | 0.00 | 0.00 |
| C I | 4890.65 | 7.49 | −2.35 | 5.5 | 7.43 | −0.08 | +0.13 | +0.02 | +0.02 | 0.00 | 0.00 |
| C I | 4932.05 | 7.69 | −1.66 | 73.1 | 8.14 | −0.07 | +0.12 | +0.03 | +0.02 | +0.07 | −0.04 |
| C I | 5017.09 | 7.95 | −2.46 | 9.6 | 8.09 | −0.07 | +0.12 | +0.03 | +0.01 | +0.01 | 0.00 |
| | 5017.05 | | −3.68 | | | | | | | | |
| C I | 5018.10 | 7.95 | −3.60 | 5.9 | 9.04 | −0.07 | +0.12 | +0.03 | +0.01 | 0.00 | 0.00 |
| C I | 5023.85 | 7.95 | −2.21 | 18.8 | 8.18 | −0.07 | +0.12 | +0.03 | +0.01 | +0.01 | −0.01 |
| C I | 5024.92 | 7.95 | −2.73 | 3.0 | 7.87 | −0.07 | +0.12 | +0.03 | +0.01 | 0.00 | 0.00 |
| C I | 5039.06 | 7.95 | −1.79 | 33.1 | 8.01 | −0.07 | +0.12 | +0.03 | +0.01 | +0.02 | −0.01 |
| | 5039.10 | | −3.20 | | | | | | | | |
| C I | 5040.13 | 7.95 | −2.30 | 13.1 | 8.10 | −0.07 | +0.12 | +0.03 | +0.01 | +0.01 | −0.01 |
| C I | 5041.48 | 7.95 | −2.00 | 52.7 | 8.16 | −0.07 | +0.12 | +0.03 | +0.01 | +0.02 | −0.01 |
| | 5041.80 | | −2.06 | | | | | | | | |
| C I | 5052.17 | 7.69 | −1.30 | 122.2 | 8.15 | −0.07 | +0.12 | +0.02 | +0.03 | +0.19 | −0.09 |
| N I | 4109.95 | 10.69 | −1.20 | 10.1 | 8.19 | +0.06 | −0.05 | −0.16 | +0.17 | +0.01 | −0.01 |
| N I | 4137.64 | 10.33 | −2.40 | 1.1 | 7.89 | +0.04 | 0.00 | −0.05 | +0.10 | 0.00 | 0.00 |
| N I | 4143.43 | 10.33 | −2.09 | 5.9 | 8.32 | +0.04 | 0.00 | −0.05 | +0.09 | +0.01 | 0.00 |
| N I | 4151.48 | 10.34 | −1.87 | 4.7 | 8.00 | +0.04 | 0.00 | −0.05 | +0.09 | 0.00 | 0.00 |
| N I | 4223.13 | 10.34 | −1.09 | 17.1 | 7.82 | +0.04 | 0.00 | −0.05 | +0.09 | +0.02 | −0.01 |
| O I | 4802.98 | 10.74 | −2.01 | 5.2 | 8.83 | +0.06 | −0.03 | −0.06 | +0.10 | +0.01 | 0.00 |
| O I | 5019.29 | 10.74 | −1.90 | 1.4 | 8.16 | +0.06 | −0.03 | −0.06 | +0.09 | 0.00 | 0.00 |
| O I | 5020.22 | 10.74 | −1.76 | 3.6 | 8.44 | +0.06 | −0.03 | −0.06 | +0.09 | 0.00 | 0.00 |
| O I | 5146.30 | 10.99 | −2.57 | 4.2 | 9.06 | +0.07 | −0.03 | −0.06 | +0.10 | 0.00 | 0.00 |
| | 5146.45 | | −2.34 | | | | | | | | |
| Ca II | 3933.66 | 0.00 | +0.13 | 138.4 | 0.26 | −0.19 | +0.22 | −0.08 | +0.11 | +0.55 | −0.15 |

Note. See the text in the Appendix for more details concerning this analysis. For those lines of He I (4026, 4471), C I (4762, 5017, 5039, 5041), O I (5146), showing fine structures due to multiplet components, the equivalent widths were measured over the whole line features and this blending effect was correctly taken into account in the abundance derivation. The meanings of the other columns are the same as in table 1.

dependence of the abundances upon the line strength or the excitation potential.

*Nitrogen* The $gf$ values were originally from Wiese et al. (1966). The abundances from individual five lines are consistent with each other.

*Oxygen* These $gf$ values originally stem the semi-empirically calculated values by Kurucz and Peytremann (1975), which are the only available source for these oxygen lines.

Because of a defect in the spectrum, we unfortunately could not measure the O I line at 3947 Å in the 2002 February data on which the present study is based. However, we clearly detect this line in another spectrum (though of poorer quality) observed in 2001 January (i.e., one year before). If we use the equivalent width of 51.7 mÅ resulting from this old spectrum, we obtain $A$(O) = 8.70 (from O I 3947 comprising three components), consistent with the present result.

*Calcium* Though a strong circumstellar component is also visible for this Ca II K line, the intrinsic stellar component of this line was rather easily identified and measured, because of the excellent matching of the radial velocity in comparison with other stellar lines. The original source of the $gf$ value is Black et al. (1972).

## References


Anders, E., & Grevesse, N. 1989, Geochim. Cosmochim. Acta, 53, 197

Bakker, E. J., Van der Wolf, F. L. A., Lamers, H. J. G. L. M, Gulliver, A. F., Ferlet, R., & Vidal-Madjar, A. 1996, A&AS, 306, 924

Black, J. H., Weisheit, J. C., & Laviana, E. 1972, ApJ, 177, 567

Bond, H. E. 1991, in Proc. IAU Symp. 145, Evolution of Stars: The Photospheric Abundance Connection, ed. G. Michaud & A. Tutukov (Dordrecht: Kluwer), 341

Bond, H. E., & Luck, R. E. 1987, ApJ, 312, 203

Cayrel, R. 1988, in Proc. IAU Symp. 132, The Impact of Very High S/N Spectroscopy on Stellar Physics, ed. G. Cayrel de Strobel & M. Spite (Dordrecht: Kluwer), 345

Fuhr, J. R., Martin, G. A., & Wiese, W. L. 1988, Atomic Transition Probabilities — Iron Through Nickel, J. Phys. Chem. Ref. Data Vol.17, Suppl. No.4 (Washington, D.C.: American Chemical Society and American Institute of Physics for National Bureau of Standards)

Giridhar, S., Lambert, D. L., & Gonzalez, G. 1998, ApJ, 509, 366

Giridhar, S., Lambert, D. L., & Gonzalez, G. 2000, ApJ, 531, 521

Giridhar, S., Rao, N. K., & Lambert, D. L. 1994, ApJ, 437, 476

Gonzalez, G., Lambert, D. L., & Giridhar, S. 1997a, ApJ, 479, 427

Gonzalez, G., Lambert, D. L., & Giridhar, S. 1997b, ApJ, 481, 452

Gonzalez, G., & Wallerstein, G. 1996, MNRAS, 280, 515

Grevesse, N., & Sauval, A. J. 1999, A&A, 347, 348

Hibbert, A., Biémont, E., Godefroid, M., & Vaeck, N. 1993, A&AS, 99, 179

Klochkova, V. G., & Panchuk, V. E. 1998, Astron. Lett., 24, 650

Kurucz, R. L. 1993, Kurucz CD-ROM, No. 13 (Harvard-Smithsonian Center for Astrophysics)

Kurucz, R. L., & Bell, B. 1995, Kurucz CD-ROM, No.23 (Harvard-Smithsonian Center for Astrophysics)

Kurucz, R. L., & Peytremann, E. 1975, Smithsonian Astrophys. Obs. Spec. Rep., No.362

Lambert, D. L., Hinkle, K. H., & Luck, R. E. 1988, ApJ, 333, 917

Luck, R. E., Bond, H. E., & Lambert, D. L. 1990, ApJ, 357, 188

Maas, T., Van Winckel, H., & Waelkens, C. 2002, A&A, 386, 504

Martin, G. A., Fuhr, J. R., & Wiese, W. L. 1988, Atomic Transition Probabilities — Scandium Through Manganese, J. Phys. Chem. Ref. Data Vol.17, Suppl. No.3 (Washington, D.C.: American Chemical Society and American Institute of Physics for National Bureau of Standards)

Monier, R., & Parthasarathy, M. 1999, A&A, 341, 117

Noguchi, K., Aoki, W., Kawanomoto, S., Ando, H., Honda, S., Izumiura, H., Kambe, E., Okita, K., et al. 2002, PASJ submitted

Sneden, C., Gratton, R. G., & Crocker, D. A. 1991, A&A, 246, 354

Takada-Hidai, M. 1990, PASP, 102, 139

Takada-Hidai, M., Takeda, Y., Sato, S., Honda, S., Sadakane, K., Kawanomoto, S., Sargent, W. L. W., Lu, L., & Barlow, T. A. 2002, ApJ, 573, 614

Van Winckel, H., Mathis, J. S., & Waelkens, C. 1992, Nature, 356, 500

Van Winckel, H., Waelkens, C., Waters, L. B. F. M., Molster, F. J., Udry, S., & Bakker, E. J. 1998, A&A, 336, L17

Waelkens, C., Van Winckel, H., Bogaert, E., & Trams, N. R. 1991, A&A, 251, 495

Waelkens, C., Van Winckel, H., Waters, L. B. F. M., & Bakker, E. J. 1996, A&A, 314, L17

Warner, B. 1968, MNRAS, 140, 53

Wasson, J. T. 1985, Meteorites: Their Record of Early Solar System History (New York: Freeman), appendix G

Wiese, W. L., Smith, M. W., & Glennon, B. M. 1966, Atomic Transition Probabilities Vol.I — Hydrogen Through Neon, NSRDS-NBS4 (Washington, D.C.: U.S. Government Printing Office)